Printed ISSN 1330–0016
Online ISSN 1333–9133
CD ISSN 1333–8390
CODEN FIZBE7

QUANTUM THEORY OF NEUTRON MULTIPLE-SLIT DIFFRACTION

XIANG-YAO WU[a,1], BAI-JUN ZHANG[a], XIAO-JING LIU[a], CHUN-LI ZHANG[a], BING LIU[a], YI-QING GUO[b], YI-HENG WU[a], YAN WANG[a] and QING-CAI WANG[a]

[a]*Institute of Physics, Jilin Normal University, Siping 136000, China*

[b]*Institute of High Energy Physics, PO Box 918(3), Chinese Academy of Sciences, Beijing 100049, China*

Received 27 August 2008; Accepted 7 October 2009
Online 29 October 2009

We study neutron multiple-slit diffraction with a quantum mechanical approach. For the double-slit diffraction, we obtain the following results: (1) when the ratio $(d+a)/a = n$ ($n = 1, 2, 3, \cdots$), orders n, $2n$, $3n$, $\cdots$ are missing in the diffraction pattern. (2) When the ratio of $(d+a)/a \neq n$ ($n = 1, 2, 3, \cdots$), there isn't any missing order in the diffraction pattern. For diffraction on N ($N \geq 3$) slits, we obtain the following results: (1) There are $N-2$ secondary maxima and $N-1$ minima between the two principle maxima. (2) As the slit number N increases, the diffraction intensity increases and the peak widths become narrower. (3) As the slit width increases, the diffraction intensity increases and the pattern width becomes narrower. (4) When the two-slit distance d increases, the number of principle maxima increases and the pattern becomes narrower. (5) We find a new quantum effect that the slit thickness c has a large effect to the multiple-slit diffraction pattern. We think all predictions in this work can be tested by neutron multiple-slit diffraction experiments.

PACS numbers: 03.75.Dg, 61.12.Bt UDC 52-656, 539.125
Keywords: matter-wave, neutron multiple-slit diffraction

1. Introduction

The wave nature of subatomic particle electron was postulated by de Broglie in 1923 and this idea can explain many diffraction experiments. The matter-wave diffraction has become a large field of interest over the last years, and it has been extended to atom and more massive, complex objects, like large molecules I_2, C_{60}

[1]E-mail address: wuxy2066@163.com

and C_{70}, which were studied in many experiments [1 – 5]. In such experiments, the incoming atoms or molecules can usually be described by plane waves. As is well known, the classical optics with its standard wave-theoretical methods and approximations, in particular those of Huygens and Kirchhoff, has been successfully applied to diffraction in optics, and has yielded good agreement with many experiments. This simple wave-optical approach also gives a description of matter wave diffraction [6 – 7]. However, matter-wave interference and diffraction are quantum phenomena, and their full description needs quantum mechanical approach.

Recently, we have studied the neutron single slit diffraction with quantum mechanical approach and obtained some important new results [8]. In this work, we study the multiple-slit diffraction of neutron with the quantum mechanical approach. In view of quantum mechanics, the neutron has the nature of a wave, and the wave is described by wave function $\psi(\boldsymbol{r}, t)$, which can be calculated with the Schrödinger wave equation. The wave function $\psi(\boldsymbol{r}, t)$ has statistical meaning, i.e., $|\psi(\boldsymbol{r}, t)|^2$ can be taken as particle's probability density at a definite position. For a multiple-slit diffraction, if we can calculate the neutron wave function $\psi(\boldsymbol{r}, t)$ distribution on a display screen, then we can obtain the diffraction intensity for a multiple-slit, since the diffraction intensity is directly proportional to $|\psi(\boldsymbol{r}, t)|^2$. In the multiple-slit diffraction, the neutron wave function can be represented into three regions. The first is the region of incoming wave where the neutron wave function is a plane wave. The second is the slit region, where the neutron wave function can be calculated using the Schrödinger wave equation. The third is the diffraction region, where the neutron wave function can be obtained by Kirchhoff's law. In the following, we calculate the wave functions in these three regions.

2. Quantum approach to neutron diffraction

We consider a multiple-slit arrangement with slit widths a, length b and the slit-to-slit distance d, as shown in Fig. 1. The x-axis is along the slit length b and the y-axis is along the slit width a. We calculate the neutron wave function in the first single slit (left) using the Schrödinger equation. Then the neutron wave function

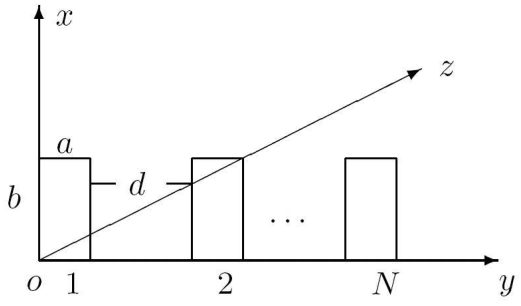

Fig. 1. N-slit geometry with a the width, b the length and d the distance between two adjacent slits.

of the second single-slit (right) can be obtained easily. At time t, we suppose that the incoming plane wave travels along the z-axis, and can be represented by

$$\psi_0(z,t) = A\exp\left(\frac{\mathrm{i}}{\hbar}(pz - Et)\right), \tag{1}$$

where A is a constant.

The potential in the single slit is

$$V(x,y,z) = \begin{cases} 0 & 0 \le x \le b, \quad 0 \le y \le a, \quad 0 \le z \le c, \\ \infty & \text{otherwise} \end{cases} \tag{2}$$

where c is the thickness of the single slit. The time-dependent and time-independent Schrödinger equations are

$$\mathrm{i}\hbar\frac{\partial}{\partial t}\psi(\boldsymbol{r},t) = -\frac{\hbar^2}{2M}\left(\frac{\partial^2}{\partial x^2} + \frac{\partial^2}{\partial y^2} + \frac{\partial^2}{\partial z^2}\right)\psi(\boldsymbol{r},t), \tag{3}$$

$$\frac{\partial^2\psi(\boldsymbol{r})}{\partial x^2} + \frac{\partial^2\psi(\boldsymbol{r})}{\partial y^2} + \frac{\partial^2\psi(\boldsymbol{r})}{\partial z^2} + \frac{2ME}{\hbar^2}\psi(\boldsymbol{r}) = 0, \tag{4}$$

where M is the mass and E the energy of the neutron. In Eq. (4), the wave function $\psi(x,y,z)$ satisfies the boundary conditions

$$\psi(0,y,z) = \psi(b,y,z) = 0, \tag{5}$$

$$\psi(x,0,z) = \psi(x,a,z) = 0. \tag{6}$$

The partial differential equation (4) can be solved by the method of separation of variables. By writing

$$\psi(x,y,z) = X(x)\,Y(y)\,Z(z), \tag{7}$$

the general solution of Eq. (3) is

$$\psi_1(x,y,z,t) = \sum_{m,n}\psi_{m,n}(x,y,z,t)$$

$$= \sum_{m,n} D_{m,n}\sin\frac{n\pi x}{b}\sin\frac{m\pi y}{a}\exp\left(\mathrm{i}\sqrt{\frac{2ME}{\hbar^2} - \frac{n^2\pi^2}{b^2} - \frac{m^2\pi^2}{a^2}}\ z\right)\exp\left(-\frac{\mathrm{i}}{\hbar}Et\right). \tag{8}$$

Equation (8) is the neutron wave function in the first single slit. Since the wave functions are continuous at $z = 0$, we have

$$\psi_0(x,y,z,t)\Big|_{z=0} = \psi_1(x,y,z,t)\Big|_{z=0}. \tag{9}$$

From Eq. (9), we obtain the coefficient $D_{m,n}$

$$D_{m,n} = \frac{4}{ab}\int_0^a\int_0^b A\sin\frac{n\pi\xi}{b}\sin\frac{m\pi\eta}{a}\mathrm{d}\xi\mathrm{d}\eta = \begin{cases} \dfrac{16A}{mn\pi^2} & m,\ n,\ odd \\ 0 & \text{otherwise}\,. \end{cases} \tag{10}$$

Substituting Eq. (10) into Eq. (8), we can obtain the neutron wave function in the first single slit,

$$\psi_1(x,y,z,t)=\sum_{m,n=0}^{\infty}\frac{16A}{an_bbm_a}\sin n_bx\ \sin m_ay\exp\left(\mathrm{i}\sqrt{\frac{2ME}{\hbar^2}-n_b^2-m_a^2}\ z\right)\exp\left(-\frac{\mathrm{i}}{\hbar}Et\right). \tag{11}$$

where $m_a = (2m+1)\pi/a$ and $n_b = (2n+1)\pi/b$.

The neutron wave function in the N-th single slit can be obtained by making the coordinate translations $x' = x,\ y' = y-(N-1)(a+d),\ z' = z$, and we can obtain the neutron wave function $\psi_N(x,y,z,t)$ in the N-th slit

$$\psi_N(x,y,z,t) = \sum_{m,n=0}^{\infty}\frac{16A}{an_bbm_a}\ \sin n_bx\ \sin m_a\big(y-(N-1)(a+d)\big)$$

$$\times\exp\left(\mathrm{i}\sqrt{\frac{2ME}{\hbar^2}-n_b^2-m_a^2}\ z\right)\exp\left(-\frac{\mathrm{i}}{\hbar}Et\right). \tag{12}$$

3. The wave function of neutron diffraction

With the Kirchhoff's law, we can calculate the neutron wave function in the diffraction area. It can be calculated by the formula [9]

$$\psi_{\mathrm{out}}(\boldsymbol{r},t) = -\frac{1}{4\pi}\int_s\frac{\exp(\mathrm{i}kr)}{r}\ \boldsymbol{n}\cdot\left[\nabla'\psi_{\mathrm{in}}+\left(\mathrm{i}k-\frac{1}{r}\right)\frac{\boldsymbol{r}}{r}\psi_{\mathrm{in}}\right]\mathrm{d}s\,, \tag{13}$$

where $\psi_{\mathrm{out}}(\boldsymbol{r},t)$ is diffraction wave function on the display screen, $\psi_{\mathrm{in}}(\boldsymbol{r},t)$ is the wave function at slit surface ($z=c$) and s is the area of the aperture of the slit. For the N-slit diffraction, Eq. (13) becomes

$$\psi_{\mathrm{out}}(\boldsymbol{r},t) = -\frac{1}{4\pi}\int_{s_1}\frac{\exp(\mathrm{i}kr)}{r}\ \boldsymbol{n}\cdot\left[\nabla'\psi_1+\left(\mathrm{i}k-\frac{1}{r}\right)\frac{\boldsymbol{r}}{r}\psi_1\right]\mathrm{d}s$$

$$-\frac{1}{4\pi}\int_{s_2}\frac{\exp(\mathrm{i}kr)}{r}\ \boldsymbol{n}\cdot\left[\nabla'\psi_2+\left(\mathrm{i}k-\frac{1}{r}\right)\frac{\boldsymbol{r}}{r}\psi_2\right]\mathrm{d}s-\ldots$$

$$-\frac{1}{4\pi}\int\limits_{s_N}\frac{\exp(\mathrm{i}kr)}{r}\;\boldsymbol{n}\cdot\left[\nabla'\psi_N+\left(\mathrm{i}k-\frac{1}{r}\right)\frac{\boldsymbol{r}}{r}\psi_N\right]\mathrm{d}s\,. \tag{14}$$

In Eq. (14), the first and N-th terms are corresponding to the diffraction wave functions of the first slit and the N-th slit.

In the following, we calculate the diffraction wave function of the first slit. It is

$$\psi_{\mathrm{out}_1}(\boldsymbol{r},t)=-\frac{1}{4\pi}\int\limits_{s_1}\frac{\exp(\mathrm{i}kr)}{r}\;\boldsymbol{n}\cdot\left[\nabla'\psi_1+\left(\mathrm{i}k-\frac{1}{r}\right)\frac{\boldsymbol{r}}{r}\psi_1\right]\mathrm{d}s\,. \tag{15}$$

The diffraction area is shown in Fig. 2, where $k=\sqrt{2ME/\hbar^2}$, s_1 is the area of the first single-slit, $\boldsymbol{r}$ is the position of a point on the surface ($z=c$), P is an arbitrary point in the diffraction area, and $\boldsymbol{n}$ is a unit vector, which is normal to the surface of the slit.

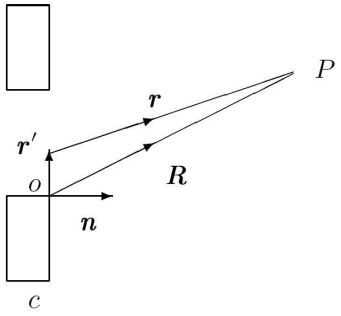

Fig. 2. Diffraction area of the single slit.

From Fig. 2, we have

$$r=R-\frac{\boldsymbol{R}}{R}\cdot\boldsymbol{r}'\approx R-\frac{\boldsymbol{r}}{r}\cdot\boldsymbol{r}'=R-\frac{\boldsymbol{k}_2}{k}\cdot\boldsymbol{r}'\,, \tag{16}$$

then

$$\frac{\exp(\mathrm{i}kr)}{r}=\frac{\exp\left(\mathrm{i}k(R-\boldsymbol{r}\cdot\boldsymbol{r}'/r)\right)}{R-\boldsymbol{r}\cdot\boldsymbol{r}'/r}=\frac{\exp(\mathrm{i}kR)\exp(-\mathrm{i}\boldsymbol{k}_2\cdot\boldsymbol{r}')}{R-\boldsymbol{r}\cdot\boldsymbol{r}'/r}$$

$$\approx\frac{\exp(\mathrm{i}kR)\exp(-\mathrm{i}\boldsymbol{k}_2\cdot\boldsymbol{r}')}{R}\qquad|\boldsymbol{r}'|\ll R\,, \tag{17}$$

with $\boldsymbol{k}_2=k\boldsymbol{r}/r$. Substituting Eq. (16) and (17) into Eq. (15), one obtains

$$\psi_{\mathrm{out}_1}(\boldsymbol{r},t)=-\frac{\exp(\mathrm{i}kR)}{4\pi R}\exp\left(-\frac{\mathrm{i}}{\hbar}Et\right)\int\limits_{s_1}\exp(-\mathrm{i}\boldsymbol{k}_2\cdot\boldsymbol{r}')\sum_{m=0}^{\infty}\sum_{n=0}^{\infty}\frac{16A}{an_b\,bm_a}$$

$$\times \exp\left(\mathrm{i}\sqrt{\frac{2ME}{\hbar^2} - n_b^2 - m_a^2}\ c\right) \sin n_b x' \ \sin m_a y'$$

$$\times \left[\mathrm{i}\sqrt{\frac{2ME}{\hbar^2} - n_b^2 - m_a^2} + \mathrm{i}\,\boldsymbol{n}\cdot\boldsymbol{k}_2 - \frac{\boldsymbol{n}\cdot\boldsymbol{R}}{R^2}\right] \mathrm{d}x'\mathrm{d}y' \,. \tag{18}$$

Assume that the angle between $\boldsymbol{k}_2$ and x-axis (y-axis) is $\frac{\pi}{2} - \alpha$ ($\frac{\pi}{2} - \beta$), and $\alpha(\beta)$ is the angle between $\boldsymbol{k}_2$ and the surface yz (xz), then we have

$$k_{2x} = k\sin\alpha\,, \qquad k_{2y} = k\sin\beta\,, \tag{19}$$

$$\boldsymbol{n}\cdot\boldsymbol{k}_2 = k\cos\theta\,, \tag{20}$$

where θ is the angle between $\boldsymbol{k}_2$ and z-axis, and the angles θ, α and β satisfy the equation

$$\cos^2\theta + \cos^2\left(\frac{\pi}{2} - \alpha\right) + \cos^2\left(\frac{\pi}{2} - \beta\right) = 1 \tag{21}$$

Substituting Eqs. (19) – (21) into Eq. (18) yields

$$\psi_{\mathrm{out}_1}(\boldsymbol{r},t) = -\frac{\exp(\mathrm{i}kR)}{4\pi R}\exp\left(-\frac{\mathrm{i}}{\hbar}Et\right)\sum_{m=0}^{\infty}\sum_{n=0}^{\infty}\frac{16A}{an_b\,bm_a}\exp\left(\mathrm{i}\sqrt{\frac{2ME}{\hbar^2} - n_b^2 - m_a^2}\ c\right)$$

$$\times \left[\mathrm{i}\sqrt{\frac{2ME}{\hbar^2} - n_b^2 - m_a^2} + \left(\mathrm{i}k - \frac{1}{R}\right)\sqrt{\cos^2\alpha - \sin^2\beta}\right]$$

$$\times \int_0^b \exp\left(-\mathrm{i}k\,\sin\alpha\,x'\right)\sin n_b x'\,\mathrm{d}x' \int_0^a \exp\left(-\mathrm{i}k\,\sin\beta\,y'\right)\sin m_a y'\,\mathrm{d}y'. \tag{22}$$

Equation (22) is the diffraction wave function of the first slit. Obviously, the diffraction wave function of the N-th slit is

$$\psi_{\mathrm{out_N}}(\boldsymbol{r},t) = -\frac{\exp(\mathrm{i}kR)}{4\pi R}\exp\left(-\frac{\mathrm{i}}{\hbar}Et\right)\sum_{m=0}^{\infty}\sum_{n=0}^{\infty}\frac{16A}{an_b\,bm_a}\exp\left(\mathrm{i}\sqrt{\frac{2ME}{\hbar^2} - n_b^2 - m_a^2}\ c\right)$$

$$\times \left[\mathrm{i}\sqrt{\frac{2ME}{\hbar^2} - n_b^2 - m_a^2} + \left(\mathrm{i}k - \frac{1}{R}\right)\sqrt{\cos^2\alpha - \sin^2\beta}\right] \times$$

$$\int_0^b \exp\left(-\mathrm{i}k\,\sin\alpha\,x'\right)\sin n_b x'\,\mathrm{d}x' \int_{(N-1)(a+d)}^{(N-1)(a+d)+a} \exp\left(-\mathrm{i}k\,\sin\beta\,y'\right)\sin m_a\big(y'-(N-1)(a+d)\big)\,\mathrm{d}y', \tag{23}$$

where d is the two slit distance. The total diffraction wave function for the N slits is

$$\psi_{\mathrm{out}}(x,y,z,t) = \psi_{\mathrm{out}_1}(x,y,z,t) + \psi_{\mathrm{out}_2}(x,y,z,t) + \cdots + \psi_{\mathrm{out}_N}(x,y,z,t)\,. \tag{24}$$

For the double-slit and three-slit diffraction, the values of N are 2 and 3. From the diffraction wave function $\psi_{\mathrm{out}}(x,y,z,t)$, we can obtain the relative diffraction intensity I on the display screen from

$$I \propto |\psi_{\mathrm{out}}(x,y,z,t)|^2 \tag{25}$$

4. Numerical results

Next, we present our numerical calculation of relative diffraction intensity. The main input parameters are $M = 1.67\times10^{-27}$ kg, $R = 1$ m, $A = 10^9$, $\alpha = 0.01$ rad, $E = 0.1$ eV, Planck's constant $\hbar = 1.055\times10^{-34}$ Js. Equations (23) – (25) are sums over the integer values m and n. We find the series are convergent when $m \geq 600$ and $n \geq 10$, so we can make numerical calculation for equations (23) – (25). We can obtain the relation between the diffraction angle β and the relative diffraction intensity I.

In the double-slit diffraction, we obtained the following results:

(1) When the ratio $(d+a)/a = n$ ($n = 1, 2, 3, \cdots$), the orders n, $2n$ and $3n$ are missing in the diffraction pattern. One can see in Fig. 3, calculated with $a = 20\lambda$, $d = 40\lambda$ and $(d+a)/a = 3$, the orders 3, 6, 9, are missing (the middle pattern is the

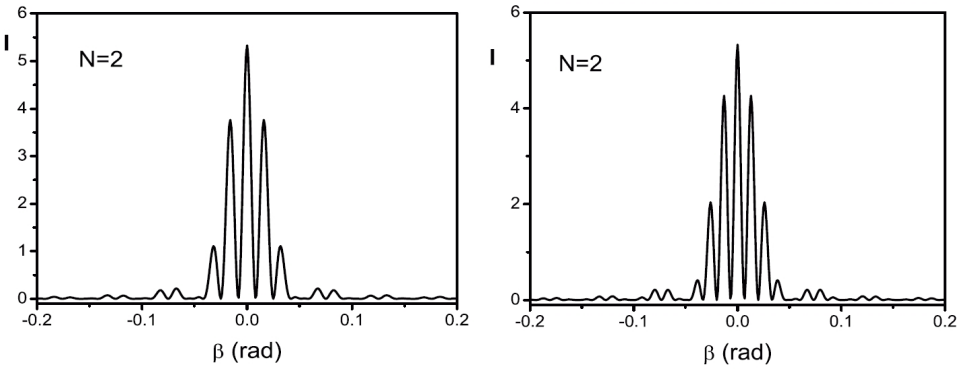

Fig. 3 (left). Relation between β and I for $a = 20\lambda$, $b = 1000\lambda$, $c = \lambda$ and $d = 40\lambda$.

Fig. 4. Relation between β and I for $a = 20\lambda$, $b = 10000\lambda$, $c = \lambda$ and $d = 55\lambda$.

zero-th order), where $\lambda = (2\pi\hbar)/\sqrt{2ME} = 1.228 \times 10^{-7}$ m is the neutron wavelength. In Fig. 5, the orders 3, 6, 9, are missing. In the double-slit diffraction, the missing order can be said to be due to a combination of interference and diffraction.

(2) When the ratio $(d+a)/a \neq n$ ($n = 1, 2, 3, \cdots$), no order is missing in the diffraction pattern. In Fig. 4, with $a = 20\lambda$, $d = 55\lambda$ and $(d+a)/a = 3.75$, (a non-integer), there isn't a missing order in the diffraction pattern. In Fig. 6, with $(d+a)/a = 3.5$, there isn't a missing order in the diffraction pattern, too.

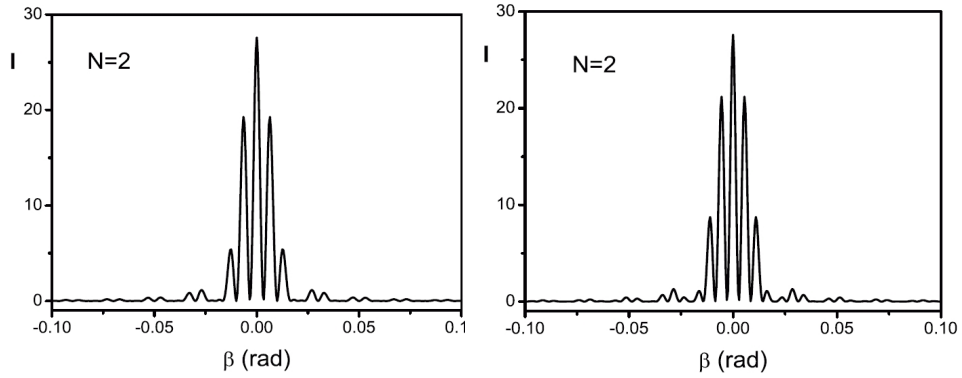

Fig. 5 (left). Relation between β and I for $a = 50\lambda$, $b = 1000\lambda$, $c = \lambda$ and $d = 100\lambda$.

Fig. 6. Relation between β and I for $a = 50\lambda$, $b = 1000\lambda$, $c = \lambda$ and $d = 125\lambda$.

(3) The slit length b has an effect on the the diffraction intensity. When b is larger, the diffraction intensity increases as can be seen in Figs. 3 and 7.

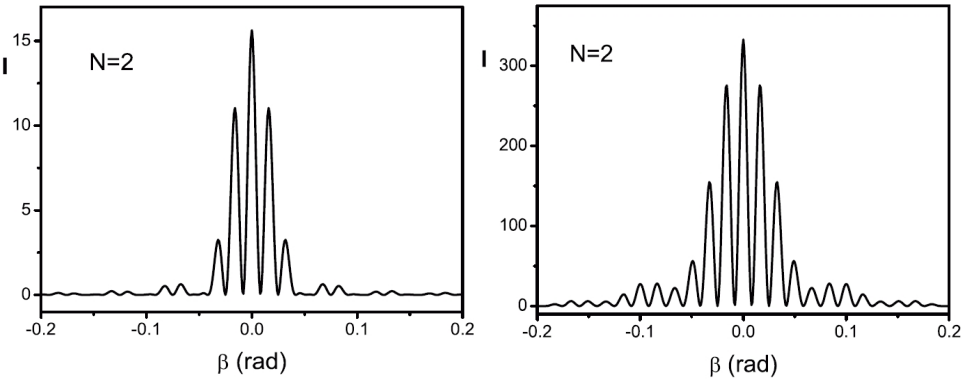

Fig. 7 (left). Relation between β and I for $a = 20\lambda$, $b = 5000\lambda$, $c = \lambda$ and $d = 40\lambda$.

Fig. 8: Relation between β and I for $a = 20\lambda$, $b = 1000\lambda$, $c = 100\lambda$ and $d = 40\lambda$.

(4) The slit thickness c has a large effect on the intensity and form of the diffraction patterns. In Figs. 3 and 8, with $(d+a)/a = 3$, the slit thickness c corresponds to 1 λ and 100 λ. The orders 3, 6, 9, $\cdots$ are missing. In Fig. 8, we find, when the slit thickness c increases, the missing-orders phenomenon disappears.

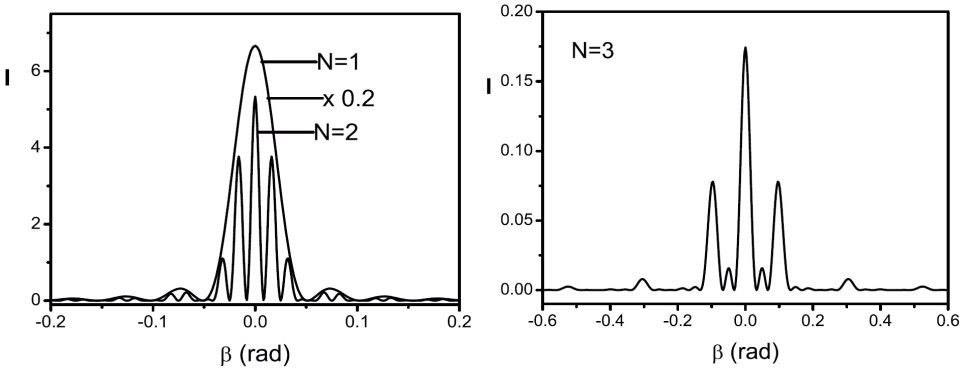

Fig. 9 (left). Relation between β and I for $a = 20\lambda$, $b = 1000\lambda$, $c = \lambda$ and $d = 40\lambda$.

Fig. 10. Relation between β and I for $a = 5\lambda$, $b = 1000\lambda$, $c = 0.1\lambda$ and $d = 5\lambda$.

Figure 9 shows the single-slit and double-slit diffraction with $a = 20\lambda$, $b = 1000\lambda$, $c = \lambda$ and $d = 40\lambda$. The real intensity I should be multiplied by 0.2.

In multiple-slit diffraction ($N \geq 3$), we obtained the results:

(1) For N-slit diffraction, there are $N-2$ secondary maxima and $N-1$ minima between the two principle maxima. Figures 10 to 14 show results for the slit number $N = 3$. There is 1 secondary maximum and 2 minima between the two principal maxima. In Figs. 10 and 14, with the ratio $(d+a)/a = 2$, the orders 2, 4, 6, $\cdots$ are missing. In Fig. 12, the ratio $(d+a)/a = 4$ and the orders 4, 8, 12, are missing. In Fig. 11, the ratio is $(d+a)/a = 2.5$ and there are no missing orders. In Fig. 13, the ratio is $(d+a)/a = 2$, but the slit thickness c was increased to $c = 10\lambda$ and there are no missing orders at 2, 4, 6, $\cdots$.

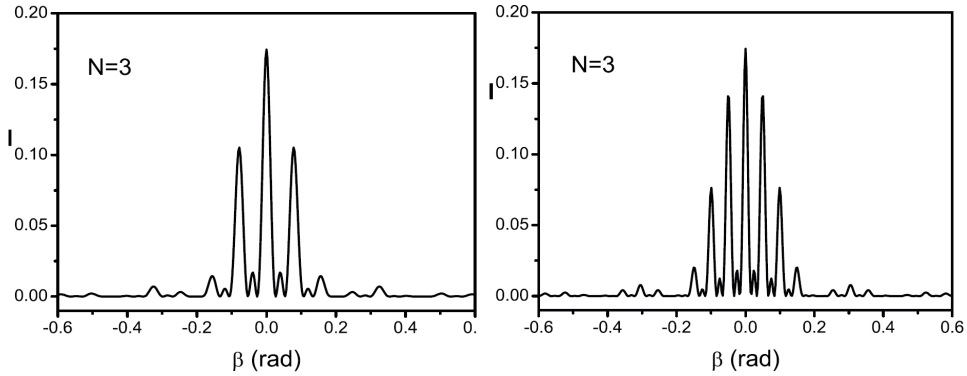

Fig. 11 (left). Relation between β and I for $a = 5\lambda$, $b = 1000\lambda$, $c = 0.1\lambda$ and $d = 7.5\lambda$.

Fig. 12. Relation between β and I for $a = 5\lambda$, $b = 1000\lambda$, $c = 0.1\lambda$ and $d = 15\lambda$.

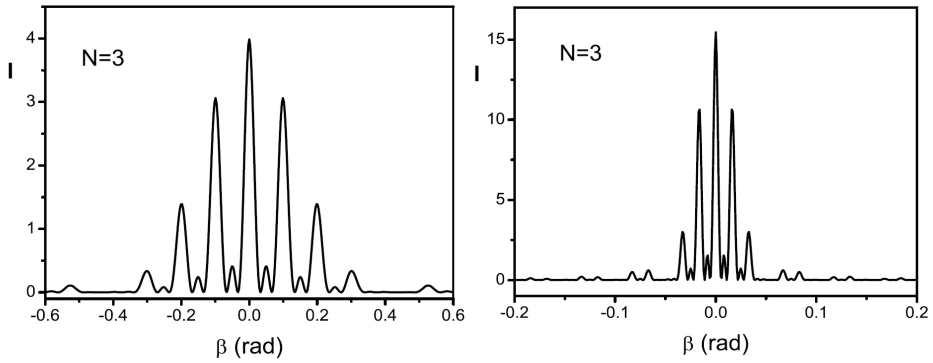

Fig. 13 (left). Relation between β and I for $a = 5\lambda$, $b = 1000\lambda$, $c = 10\lambda$ and $d = 5\lambda$.

Fig. 14. Relation between β and I for $a = 20\lambda$, $b = 1000\lambda$, $c = \lambda$ and $d = 40\lambda$.

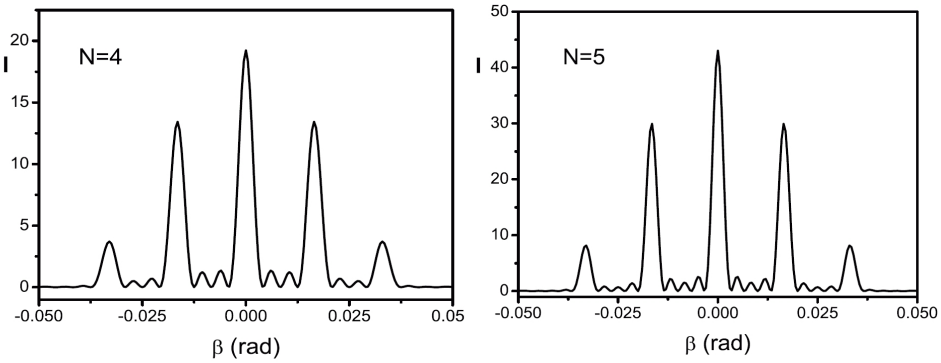

Fig. 15 (left). Relation between β and I for $a = 20\lambda$, $b = 1000\lambda$, $c = \lambda$ and $d = 40\lambda$.

Fig. 16. Relation between β and I for $a = 20\lambda$, $b = 1000\lambda$, $c = \lambda$ and $d = 40\lambda$.

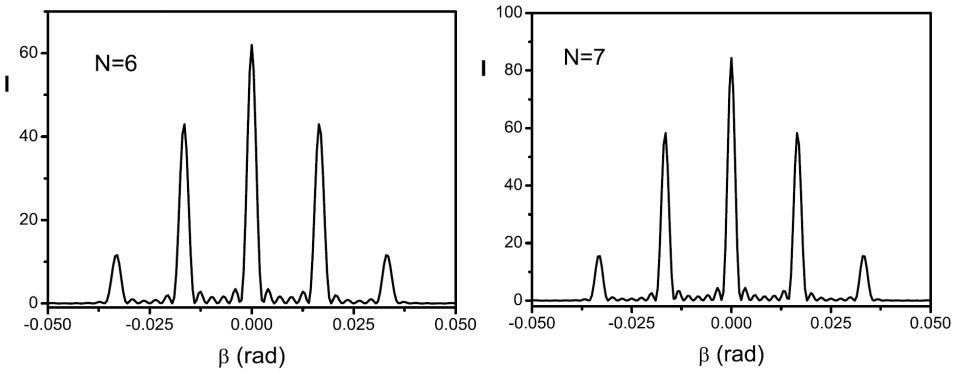

Fig. 17 (left). Relation between β and I for $a = 20\lambda$, $b = 1000\lambda$, $c = \lambda$ and $d = 20\lambda$.

Fig. 18. Relation between β and I for $a = 20\lambda$, $b = 1000\lambda$, $c = \lambda$ and $d = 40\lambda$.

(2) Comparing Fig. 10 with Fig. 14, we can find that the diffraction intensity increases and the pattern width becomes narrower when the slit width a increases.

(3) From Figs. 14 to 20, we can find that the diffraction intensity increases and the pattern width becomes narrower when the slit number N increases.

(4) There are $N-2$ secondary maxima and $N-1$ minima between the two principle maxima, as can be found from Fig. 14 to Fig. 20.

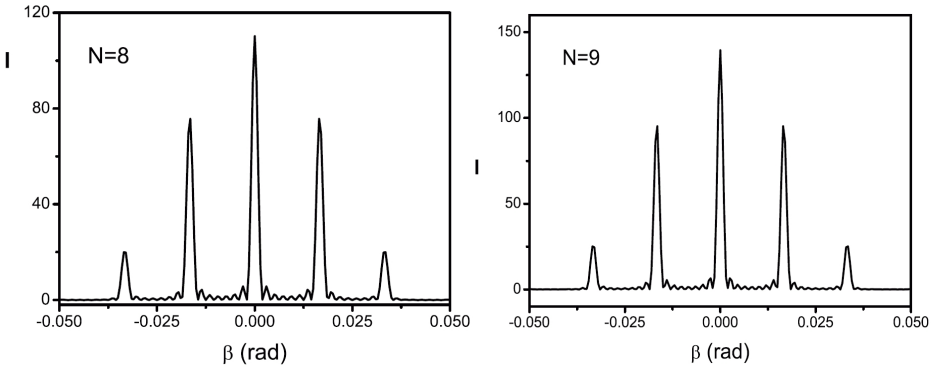

Fig. 19 (left). Relation between β and I for $a = 20\lambda$, $b = 1000\lambda$, $c = \lambda$ and $d = 40\lambda$.

Fig. 20. Relation between β and I for $a = 20\lambda$, $b = 1000\lambda$, $c = \lambda$ and $d = 40\lambda$.

5. *Conclusion*

We present the results of calculations of neutron multiple-slit diffraction based on the quantum mechanical approach.

For the double-slit diffraction, we obtain the following results: (1) When the ratio is $(d+a)/a = n$ ($n = 1, 2, 3, \cdots$), the orders n, $2n$, $3n$, $\cdots$ are missing in the diffraction pattern. (2) When the ratio is $(d+a)/a \neq n$ ($n = 1, 2, 3, \cdots$), no order is missing in the diffraction pattern.

For N-slits diffraction ($N \geq 3$), we obtain the following results: (1) missing orders similar to the double-slit diffraction also appear. (2) There are $N-2$ secondary maxima and $N-1$ minima between the two principal maxima. (3) As the slit number N increases, the diffraction intensity increases and the pattern width becomes narrower. (4) As the slit width a increases, the diffraction intensity increases and the pattern width becomes narrower. (5) When the two slit distance d increases, the number of principle maxima increases and the pattern becomes narrower. (6) We find a new quantum effect that the slit thickness c has a large effect to the multiple-slit diffraction pattern. We think all the predictions in our work can be tested by the neutron multiple-slit diffraction experiments.

References

[1] O. Carnal and J. Mlynek, Phys. Rev. Lett. **66** (1991) 2689.

[2] W. Schöllkopf and P. J. Toennies, Science **266** (1994) 1345.

[3] M. Arudt, O. Nairz, J. Voss-Andreae, C. Kwller, G. Vander Zouw and A. Zeilinger, Nature **401** (1999) 680.

[4] O. Nairz, M. Arudt and A. Zeilinger, J. Mod. Opt. **47** (2000) 2811.

[5] S. Kunze, K. Dieckmann and G. Rempe, Phys. Rev. Lett. **78** (1997) 2038.

[6] B. Brezger, L. Hackermuller, S. Uttenthaler, J. Petschinka, M. Arndt and A. Zeilinger Phys. Rev. Lett. **88** (2002) 100404.

[7] S. A. Sanz, F. Borondo and J. M. Bastiaans, Phys. Rev. A **71** (2005) 042103.

[8] X. Y. Wu, J. H. Yang, X. J. Liu, L. Wang, G. Liu, X. H. Fan and Y. Q. Guo, Chin. Phys. Lett. **24** (2007) 1813.

[9] J. D. Jackson, *Classical Electrodynamics*, John Wiley & Sons, Chichester, Ch. 10 (1999) p. 579.

KVANTNA TEORIJA DIFRAKCIJE NEUTRONA NA MNOGO PUKOTINA

Proučavamo difrakciju neutrona na mnogo pukotina kvantno-mehaničkim pristupom. Za dvije pukotine postigli smo ove ishode računa: (1) Kada je omjer $(d + a)/a = n$ ($n = 1, 2, 3, \cdots$), izostaju redovi n, $2n$, $3n$, $\cdots$ u difrakcijskoj slici. (2) Kada je $(d + a)/a \neq n$ ($n = 1, 2, 3, \cdots$), svi se redovi javljaju u difrakcijskoj slici. Za difrakciju na N ($N \geq 3$) pukotina dobili smo ove ishode: (1) Između dva osnovna maksimuma javljaju se $N - 2$ sekundarna maksimuma i $N - 1$ minimuma. (2) Kako se broj pukotina povećava, povećava se intenzitet difrakcijske slike i širine vrhova se smanje. (3) Kad se širina pukotina poveća, pojača se intenzitet difrakcije a vrhovi se suze. (4) Ako se poveća razmak pukotina d, poveća se broj glavnih maksimuma i oni se suze. (5) Nalazimo nov kvantni efekt da duljina pukotina c ima velik utjecaj na difrakcijsku sliku u slučaju mnogo pukotina. Vjerujemo da će se ishodi ovog rada provjeriti mjerenjem neutronske difrakcije na rešetci s mnogo pukotina.